Chapter-6

A Comparative study of the catalytic behavior of $PrBaCo_2O_{6-\delta}$ and $Pr_{1.6}Ba_{0.4}Co_2O_{6-\delta}$: bulk and thin film

Publication: ***Ajay S. Bangwal, Manisha Chauhan and Prabhakar singh***, *"A comparative study of the catalytic behavior of $PrBaCo_2O_{6-\delta}$ and $Pr_{1.6}Ba_{0.4}Co_2O_{6-\delta}$: bulk and thin fim (to be communicated)*

CHAPTER 6: A Comparative study of catalytic behavior of $PrBaCo_2O_{6-\delta}$ and $Pr_{1.6}Ba_{0.4}Co_2O_{6-\delta}$: Bulk and thin film

6.1 Introduction

In the previous chapter, the impact of oxygen reduction (ORR) and Oxygen evolution reaction (OER) in the performance of many electrochemical devices and storage system has been already discussed. ORR refers to the reduction half reaction whereby O_2 is reduced to water in fuel cells. OER is the cathodic reaction for water electrolyzers. In case of metal-air batteries and rechargeable fuel cell, OER act as an anodic reaction. Energy loss in OER is much higher than HER. OER is a difficult process that involves four-electron coupled electron transfer and formation of oxygen-oxygen bond. ORR and OER are kinetically unfavorable and requires a catalyst to accelerate the reaction.

Oxygen reduction/evolution electrocatalyst has been developed for a long time. Initially, noble metal based on Pt, Pd, Au and their alloys were considered as important ORR/OER catalyst. After that, first-raw transition metal oxide such as Co, Ni, Mn, and Fe have been extensively researched for their relatively good catalytic activity for OER. Research was then shifted towards perovskites-based ORR/OER catalyst. Oxide based electrocatalysts, particularly double perovskites have been reported as potential alternative to the metal electrodes for ORR and OER in neutral, alkaline, and acidic medium. The majority of the work is dedicated to discovering materials with low overpotential as well as the investigation of activities and reaction mechanism. However, the subject of chemical stability and degradation mechanism of ORR/OER electrocatalyst received less attention, without mass loss as well as structural and chemical alterations being taken into account[222].

Another foremost objective of catalyst research is to design and adjust catalytic activity and selectivity by altering structural features. Another significant aspect to contemplate, particularly in the case of heterogeneous catalysts, is how catalyst materials are incorporated into catalyst reactors. For all of these devices, thin oxide films as designable catalysts and catalyst supports are vital for controlling the functional characteristics and, thus, the intrinsic catalyst properties of the catalytic species deposited into them[223].

In pervious chapter, double perovskite $PrBaCo_2O_{6-\delta}$ and its compositions has been studied in details for their suitability as catalyst for ORR and OER. In continuation of the previous chapter, $Pr_{1.6}Ba_{0.4}Co_2O_{6-\delta}$ (x =0.6) along with the $PrBaCo_2O_{6-\delta}$ (x =0) has been choosen for further study. In this chapter, two samples are designed in thin film and their comparative study of their catalytic study is performed in bulk and thin film.

6.2 Synthesis and characterization

Thin film technology, which was used in this work, is a highly fascinating approach for electrocatalysis. Both the traget for deposition, $PrBaCo_2O_{6-\delta}$ and $Pr_{1.6}Ba_{0.4}Co_2O_{6-\delta}$ was prepared by the solid state route menthod maintaining the optimization conditions same as mentioned in previous chapters. Thin film was grown on the silica substrate using the KrF excimer laser (λ= 248nm). The dimensions of the substarte was 1.5 cm × 1.0 cm × 2 mm. The power of the laser was 430 mJ for depositions in both thin films. The film was deposited at 700 °C and the shot of deposition was 1000 in each case.

The phase formation in thin film was checked by EQUINOX Laue X-ray diffractometer. Deposition of thin film was checked by optical microscope, which was further confirm by AFM by using the NTEGRA Prima instrument. The catalytic study of the sample was

performed through cyclic voltammetry using Kethley 2450 source meter using three-electrode system. For three electrode system, Pt wire was used as counter electrode, Ag/AgCl was used as reference electrode. For working electrode, thin film was attached with copper wire making it insulating from outside. The concentration of electrolyte solution was 1 M sodium sulfate (Na_2SO_4).

6.3 Results and Discussion

6.3.1 Structural Studies

The XRD pattern of each thin film was recorded at a particular incident angle and shown in figure 6.1. A major peak is observed at 32.57°, with indexing of (102) for x=0.6 assositaed with $Pr_{1.6}Ba_{0.4}Co_2O_{6-\delta}$[224]. Another peak is observed at 58.50° in both of the sample with indexing (104)[152], [224]. Thus, XRD study confirms the phase formation in both thin films.

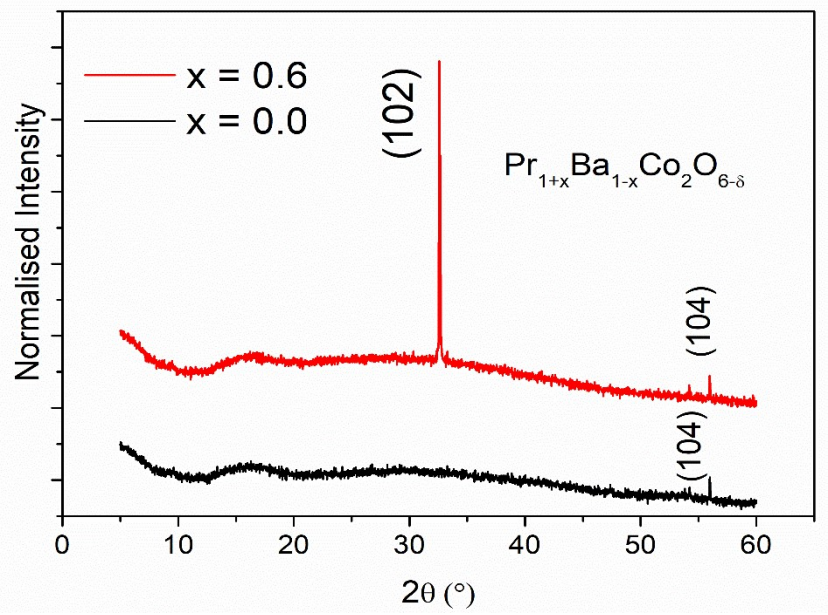

Figure 6.1: X-ray diffraction pattern of x = 0 and x = 0.6 thin film

.

6.3.2 Optical microscopy observation and Surface morphology

Figure 6.2 shows the optical micrograph of some area of the both thin films. The magnitude of the area was kept fixed throughout this study. The deposited x=0 and x=0.6 form different island irregular in size and shape. The dark region in figure indicating the deposition on thin film on substrate. Topographical images are recorded through AFM is shown in figure 6.3, suggested that obtain thin films have the square shaped morphology.

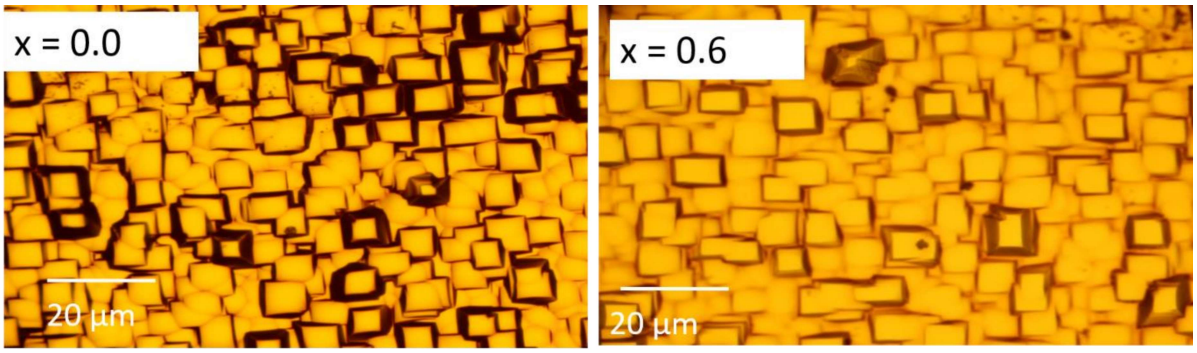

Figure 6.2: Optical microscopy images of x=0 and x=0,6 thin film

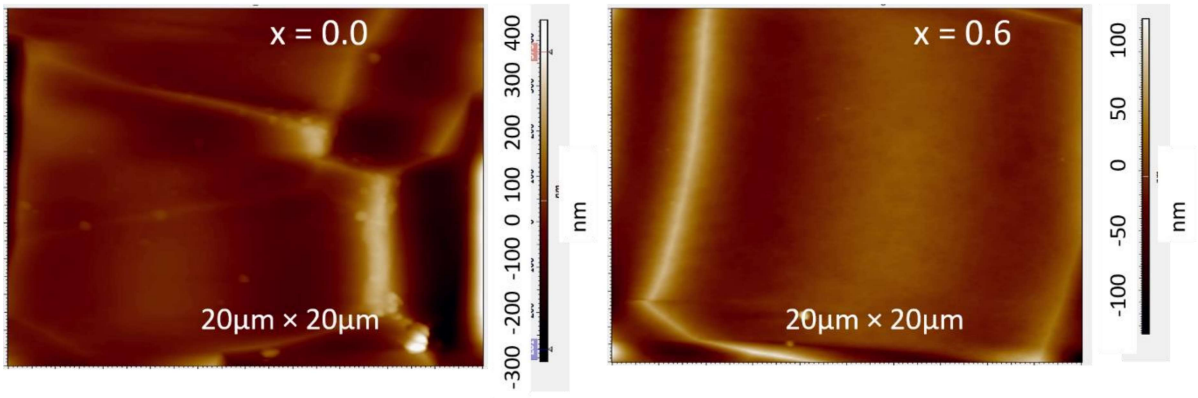

Figure 6.3: Topographical AFM images of x=0 and x=0.6 thin film

6.3.3 Catalytic Studies

6.3.3.1 Cyclic Voltammetry

The electron transfer phenomenon is analyzed using cyclic voltammetry. Scan rate is a key parameter in cyclic voltammetry. CV was studied at different scan rate and figure 6.4 shows the CV curve at 50mV/s scan rate. It can be seen in Fig. 6.4 that the "duck" shaped cyclic voltametric curve is obtained for all the samples. These duck shaped curves are a sign of catalytic regeneration of reactant near electrode However, when assessing a bulk sample to a thin film, the cathodic current is higher in the bulk sample. In the x=0.6 bulk sample, the highest cathodic current is noticed. Additionally, when compared to the other samples, the area under the curve for x = 0.6 (bulk) is larger. In addition to "duck" shaped feature, there is absence of kink in the curves of the thin film. This kink symbolizes the presence of multiple oxidation states that may be interconverted via electron transfer.

The variation of scan rate for the examined samples are depicted in figure 6.5. It is observed that with the variation of scan rate, the peak position is found to move towards higher current and higher voltages. The increase in current with the scan rate is a common observation is basically due to the reduction in the size of diffusion layer as the scan rate increases. At higher scan rate, kink is present in the (x=0) bulk sample. Peak-to-peak separation seems to shift with the scan rate in all the samples, confirming one electron transfer between the analyte and the electrode

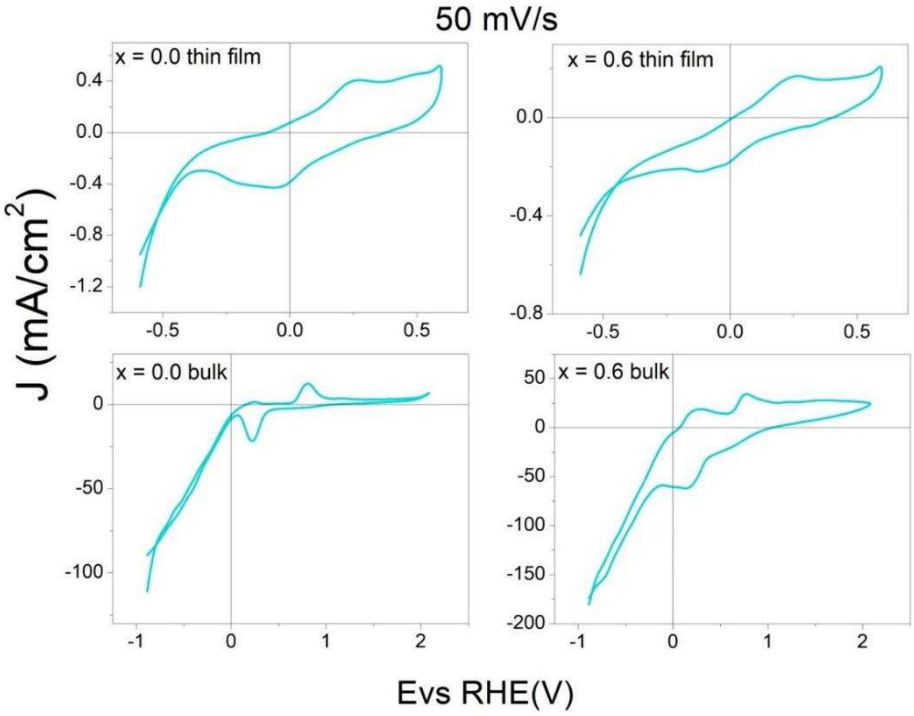

Figure 6.4: Cyclic Voltammetric curves for the x=0 and x=0.6 (bulk and thin film) at scan rate of 50 mV/s

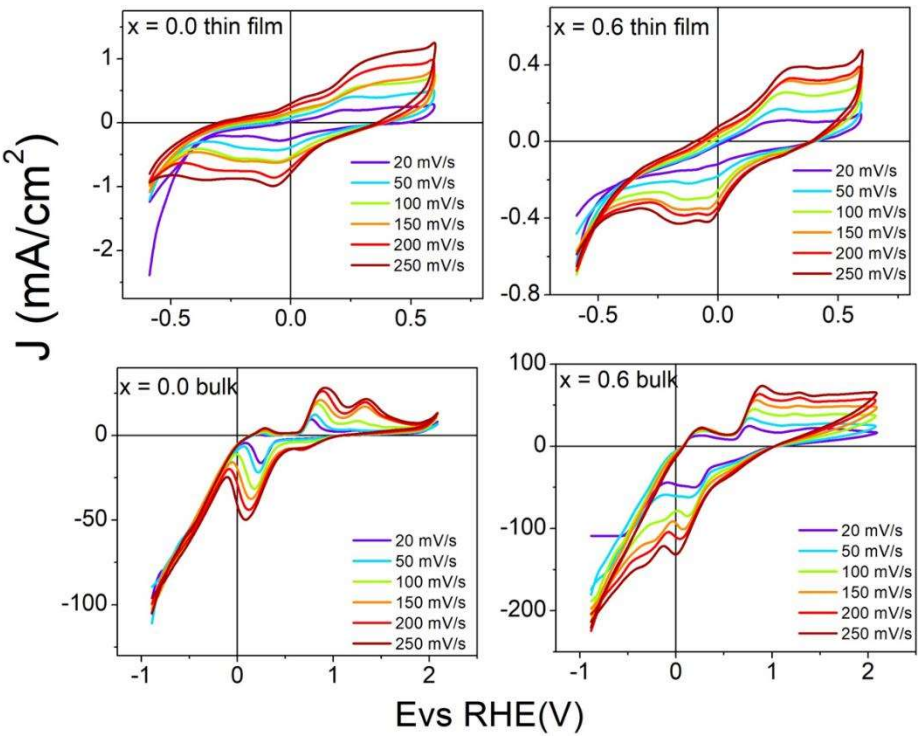

Figure 6.5: Cyclic Voltammetric curves for the x=0 and x=0.6 (bulk and thin film) at different scan rate

6.3.3.2 RS equation

Randles-Selvick (RS) equation, $i_p = 0.446nFAC^0\left(\frac{nF\upsilon D_o}{RT}\right)^{1/2}$ is employed for electrochemically reversible process with the freely involved redox carriers. For electron adsorbed species, this equation is modified as $i_p = \frac{n^2F^2}{4RT}\upsilon A\Gamma^*$ where n is number of electrons involved in the redox reaction, F is faraday constant, υ is scan rate, R is gas constant, T is Temperature in Kelvins, A is electrode surface area, D_o is diffusion coefficient and C^0 is the bulk concentration and Γ^* is the surface covered under adsorbed surfaces[225]. To describe peak behavior, peak current is plotted versus $v^{1/2}$ (Fig.6.7). The plot of RS equation is linear for all the sample, indicating the quasi-electrochemical reversibility with the freely diffusing redox species.

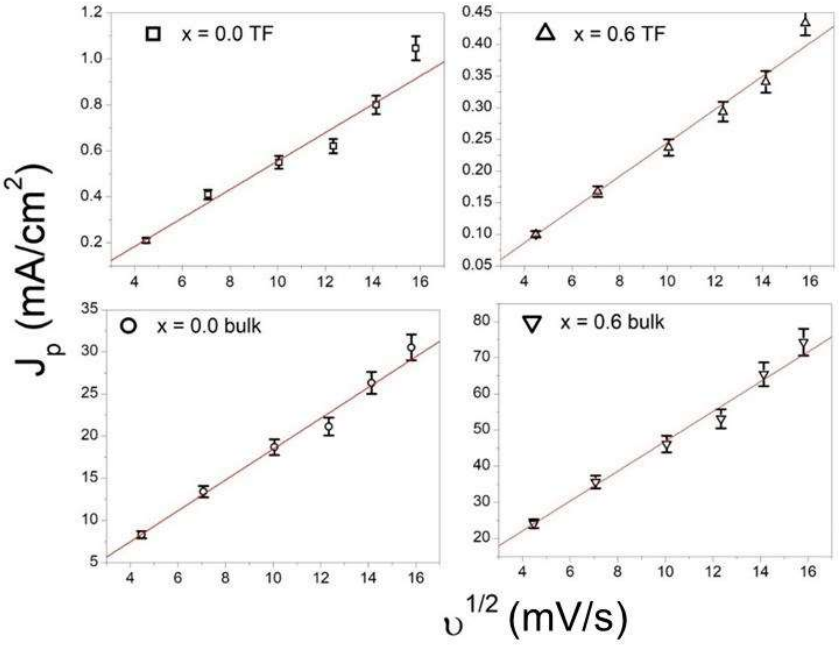

Figure 6.7: Variation of i_p vs $v^{1/2}$ as per RS equation for all the sample

6.3.3.3 Chronoamperometry study

The chronoamperometric response of the all the compositions is used to evaluate transient current decay time (Fig. 6.8). The transient current decay time is estimated by fitting the current vs time graph (Fig.6.8) with the exponential decay equation. For the bulk sample, the decay time is already calculated and mentioned in previous chapter. In case of thin film, the decay time is same as that of bulk in case of x=0.6 and observed to be ~0.76 sec. On the other hand, decay time differ significantly for x=0 thin film. The decay time is reduced by 70 times in case of thin film as compared to the bulk sample. For x=0 thin film, the decay time is 10.86 seconds. For electrode materials, the transient response should be very less, often of the order of 1 sec. Because of its lower transient response and electrochemical reversibility with freely diffusing species, the sample x = 0.6 (thin film) is also suited for the electrode.

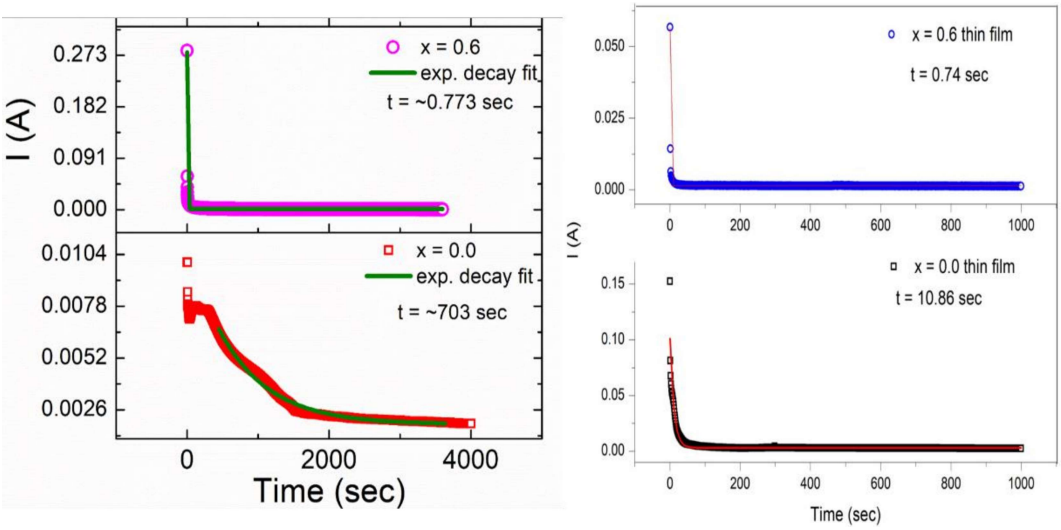

Figure 6.7: Chronoamperometric response for x = 0 and x = 0.6 (bulk and thin film)

6.4 Conclusion

Thin film of two optimized electrode $PrBaCo_2O_{6-\delta}$ and $Pr_{1.6}Ba_{0.4}Co_2O_{6-\delta}$ was synthesized using pulse laser deposition techniques and their catalytic properties was investigated. The conclusion of their catalytic behavior is shown in Fig. 6.8. It can observe easily that current is too much higher in case of bulk sample as compared to the thin film. However, value of current is also significant in case of thin film as well. Transient response time become better in thin film as compared to bulk sample and on the basis of catalytic behaviors for x=0.6, thin film can be proposed as a suitable catalyst for ORR.

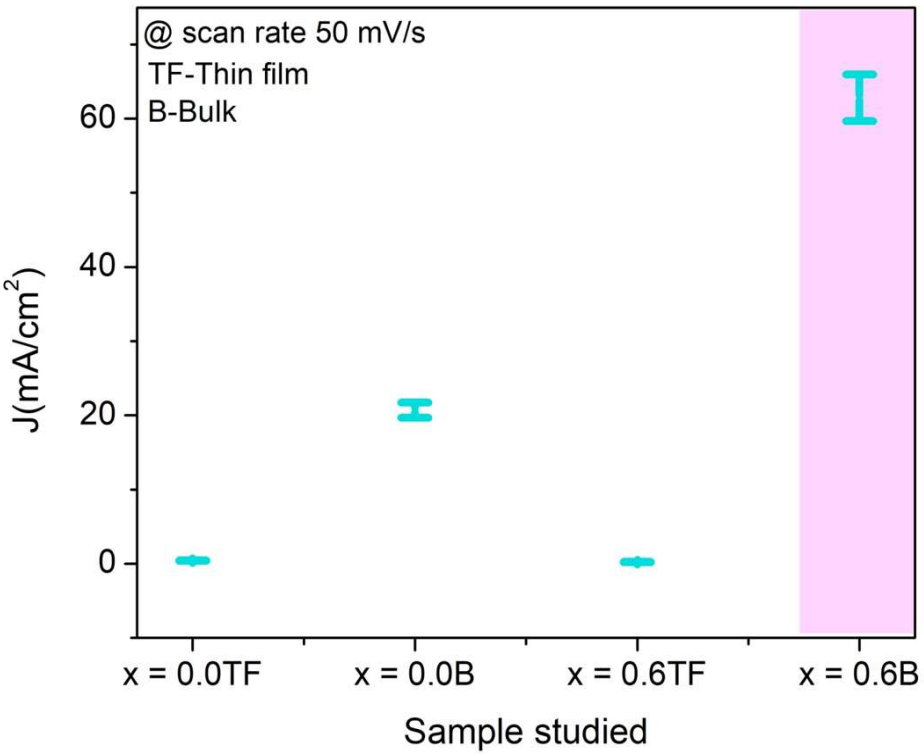

Figure 6.8: Comparative of current observed in all the studied samples